Supplementary Information for
Arbitrary and Active Colouring of Solar Cells with Negligible Loss of Efficiency

by
Yan-Song Zhang, Hasan Arif Yetkin, Hakam Agha, Sevan Gharabeiki, Rijeesh Kizhakidathazhath, Lena Merges, Ricardo G. Poeira, Jan P.F. Lagerwall, and Phillip J. Dale

1 Solar Cell with Single Colour Cholesteric Liquid Crystal

1.1 Chemical Formulation of CLC for Single Colour Solar cells

The different monomers used to create single spectral colour CLC mixtures are shown in Fig. S1. It contains bifunctional polymerizable mesogen RM257, monofunctional polymerizable monomer 6OCB-1-ene, right-handed chiral dopant R5011 and photoinitiator IRG651.

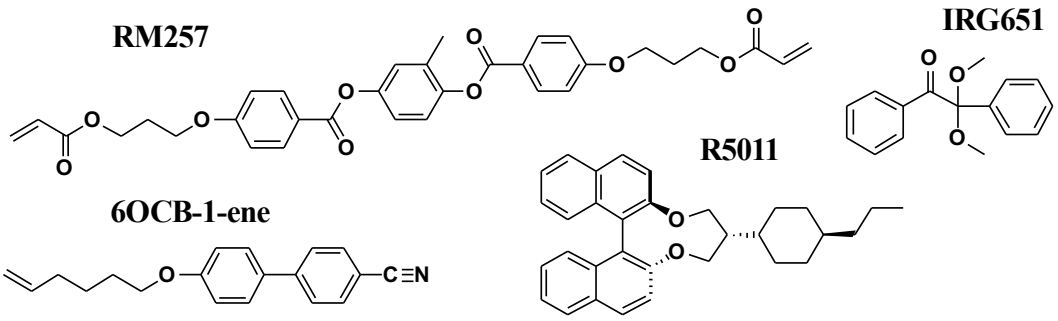

Figure S1. Chemical structures of monomers used to prepare the permanent single colour films.

The exact compositions for blue, green and red colours are given below in Table S1. The main difference is the amount of chiral dopant R5011 that is used. By reducing the weight percent of the R5011 chiral dopant in the mixture, the single spectral colour is shifted from blue to red.

Table S1. Compositions of CLC mixtures used to prepare the permanent single colour films.

Colour	RM257 (wt.%)	6OCB-1-ene (wt.%)	R5011 (wt.%)	Irg651 (wt.%)
Blue	40	56.35	2.65	1
Green	40	56.70	2.30	1
Red	40	57.15	1.85	1

The permanent single colour solar cells are prepared with the procedure depicted in Fig. S2: The three CLCs are mixed according to the proportions in Table S1 and then placed in three sample vials. Then all the mixtures are magnetically stirred at 500 rpm and 80 °C (isotropic phase) for around 5 h to ensure that all the components are homogeneously mixed. The mixtures are cooled to 40 °C to bring them into cholesteric phase. We keep stirring at 500 rpm at this temperature for 1 h before use. The protective top glass plates are placed on eight adjacent solar cells each, using glue along two parallel sides of each plate. By including spacer balls in the glue we fixed the solar cell-to-protective glass spacing to 15μm. The three CLC mixtures are filled by capillary force at 40 °C from an edge without glue. After the entire area of each cover plate is filled, the samples are cured by UV photopolymerisation at room temperature.

1.2 Current-Voltage Measurements

Fig. S2e shows the real image of the blue coloured solar cells. Fig. S2f depicts electrical and opto-electronic characterisation procedures of the solar cells before and after CLC coating. As there is no single, unique reference solar cell for performance comparison across all coloured cells, each solar cell prior to CLC coating is treated as its own reference. Consequently, solar cell performance comparisons are conducted by evaluating each solar cell individually before and after CLC. Thus, for each cell, the uncoloured state “before CLC” serves as the reference for evaluating any changes in performance due to the addition of the CLC coating. Accordingly, in the case of "before CLC" *JV* and *EQE* (the *EQE* spot is indicated with a yellow dot) measurements have been performed on all solar cells before CLC coating. After implementing the CLC coating, *JV* and *EQE* have been measured on all solar cells. As described in the Methods for *JV*-measurement, based on the J_{SC}^{EQE} derived from the respective *EQE* spectrum, all *JV*-curves have been corrected, enabling to calculate the active area efficiencies of the solar cells.

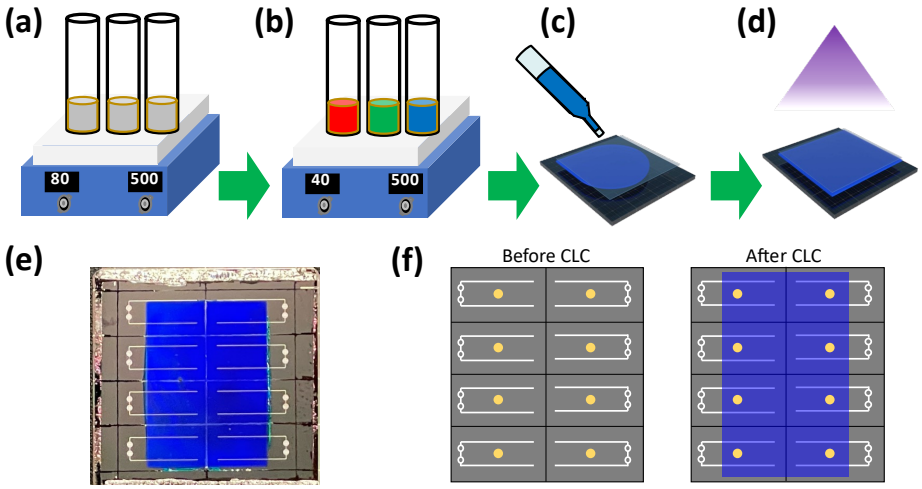

Figure S2. Schematic of the procedure for fabricating permanent CLC-generated single spectral colour solar cell. Stirring until homogeneous at 500 rpm and (a) 80 °C for 5 h, (b) cooled to 40 °C and mixing for a further 1 h. (c) Filling the mixtures at 40 °C and (d) UV curing the samples at room temperature. (e) Photograph of blue coloured CLC film-covered solar cells. (f) It depicts the characterization procedures before and after CLC colouring. Before CLC, *JV* and *EQE* (location of *EQE* spot is shown with yellow dot.) have been measured on all solar cells. After CLC colouring, again *JV* and *EQE* measurements have been performed. Based on the J_{SC}^{EQE}, all *JV*-curves have been corrected, thereby correcting the corresponding PCEs.

1.3 *JV*-curves of Permanently Coloured Solar Cells Before and After *EQE* Correction

Fig. S3 shows the measured illuminated *JV*-curves of the best solar cells. Importantly, measured *JV* data exhibit the same trend observed after the correction of J_{SC}^{JV} with J_{SC}^{EQE}. It is worth noting that the light intensity of the sun simulator has a tolerance of ±2%. The *JV* data require *EQE* correcting because the CLC layer does not fully cover the total area of the solar cell.

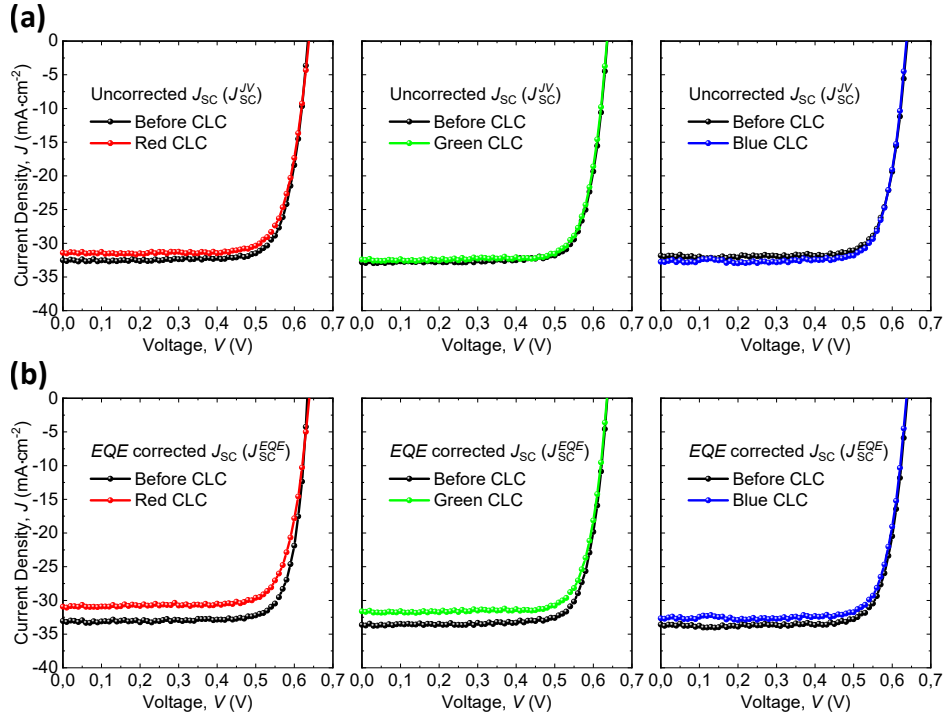

Figure S3. *JV*-curves of the best solar cells before and after permanent CLC colouring shown in Fig. 2 (a) without and (b) with J_{SC}^{EQE} correction.

1.4 Statistical Analysis of Performances for Permanently Coloured Solar Cells

Fig. S4 shows the statistical analysis of performances of solar cells after colouring with red, green and blue in comparison to the before CLC colouring, demonstrated in Fig. 2. Regrettably, several of the solar cells used for the red and blue substrates were either covered with CLC over the contacts or shorted, and thus have less than eight cells. The boxplot graph shows the distribution of PCEs of solar cells with the box indicating the interquartile range (25% to 75%), the whiskers extending to 1.5 times the interquartile range. The median is shown by a central line, while the mean is indicated with a square. Any outliers are shown as diamonds. Overall it can be seen that CLC coating did not unduly affect any of the solar cells electrical performance.

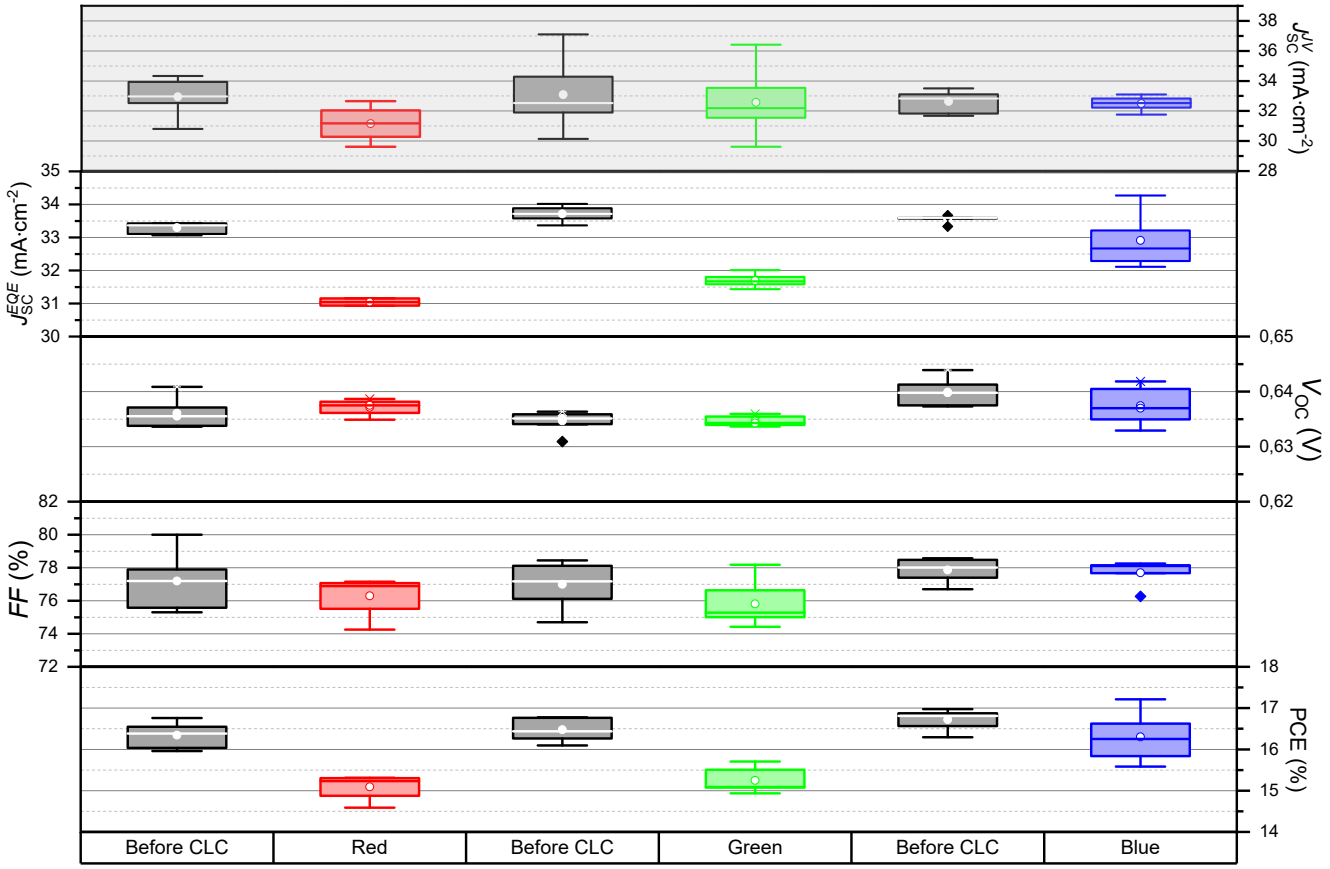

Figure S4. Boxplot of the *JV* parameters of four red, eight green and five blue solar cells before and after CLC colouring layers for the statistical analysis together with J_{SC}^{JV} and J_{SC}^{EQE}. It is important to note that all the PCEs and *FF* are recalculated according to J_{SC}^{EQE}.

1.5 Effect of Air and Cover Glass on the *EQE*-Spectra of Solar Cells

Fig. S5 shows the *EQE* spectra of a reference (uncoated) CIGSe solar cell, which is shown in Fig. 3, before and after placing a protective cover glass on top in order to show the effect of cover glass. A drop in current collection across all wavelengths can be observed from the addition of the glass leading to a 2.6 mA.cm^{-2} reduction in J_{SC} due to reflection from the upper glass surface and to bad refractive index matching (solar cell - air - cover glass), proving that the CLC between the cover glass and the solar cell behaves as a good refractive index matching layer (see Fig. 2b).

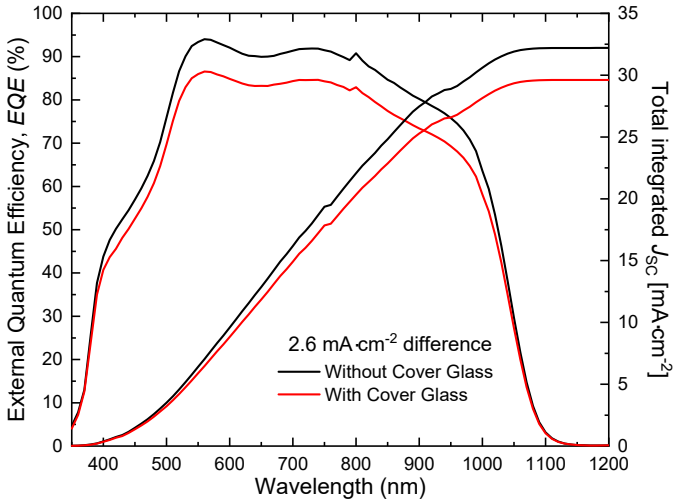

Figure S5. *EQE*-measurements on a normal black coloured solar cell without and with cover glass in order to see the adverse effect of a cover glass and interstitial air layer, leading to higher reflection due to bad refractive index matching.

1.6 Comparison of Reflection Spectra of Colouring Layers from Various Technologies

Fig. S6 presents a comparative analysis of the reflection spectra of three colouring technologies. Our CLCs exhibit the highest reflection, at approximately 48 %, which is close to the maximum reflection for a single layer CLC. Additionally, the reflection band width of our CLCs is considerably broader and in a rectangular shape, which is typical for CLCs, rather than Gaussian. It is worth noting that the reflection band width of CLCs can be narrowed down by fine-tuning the chemical composition.

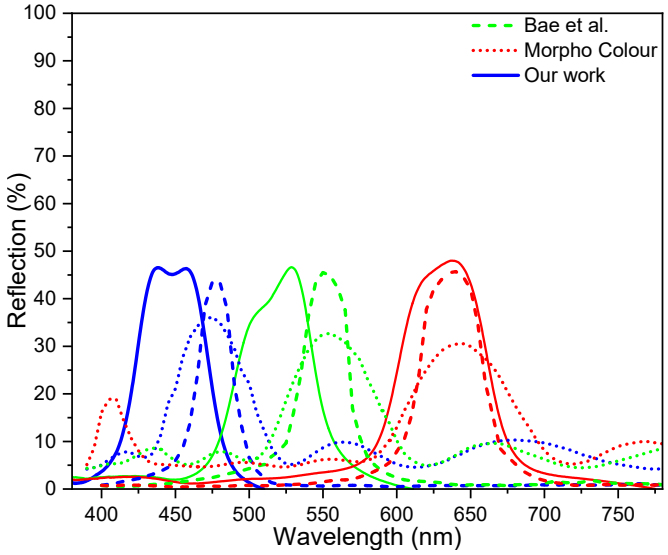

Figure S6. Comparison of the reflection spectra of all the single colour layers obtained from Morpho Colour[10] and Bae et al.[21] (digitised and replotted here) with those of our single coloured solar cells.

1.7 Thermal Stability of Polymerised CLCs

The thermal stability of single spectral colour films on solar cells was assessed by subjecting samples to a temperature range of 20 to 120 °C. Each colour film is investigated by POM and reflection spectra during heating to different temperatures and kept for one hour, using a Linkam heating stage operating at a heating rate of 1°C/min. At temperatures below 100 °C, no discernible colour shifts are observed in the CLC films, as shown in Fig. S7. Beyond 100 °C, the retroreflection experienced a minimal shift of less than 5 nm. Additionally, both POM and direct visual observation do not reveal any noticeable colour change.

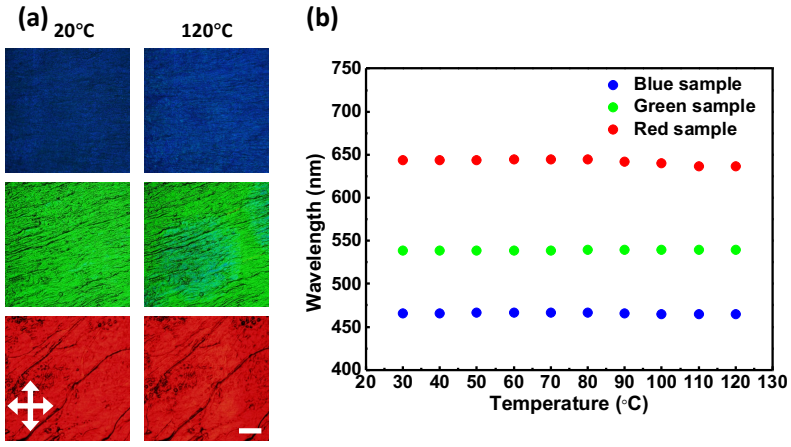

Figure S7. (a) Reflection POM images of blue, green and red colour solar cells heating from 20 to 120 °C. (b) Record reflection spectra. Scale bar: 200μm.

An environmental stability experiment was carried out on a CLC film subjected to a temperature of 85°C and 85% humidity. The experimental setup is illustrated in Fig. S8. Humidity was maintained at 85% using a dew-point generator and monitored by a computer using an electronic humidity sensor. The sample was kept on a heating plate to ensure a temperature of 85°C, as confirmed by monitoring with an infrared camera, see Fig. S9. The test sample consists of a CLC film with red retroreflection enclosed between glass slides, separated by 10 μm spherical spacers, with UV-cured glue applied at the four corners to mechanically stabilise the structure. The CLC precursor was introduced via capillary action and then polymerised using UV light. The sample was placed in the humidity chamber and its spectral response was continuously monitored. Fig. 2f shows the results of the 10-day environmental stability test. The CLC film still maintains good optical properties in high-temperature and high-humidity environments. A temperature-sensitive CLC film was also tested in this environment for five days (see Fig. 5d).

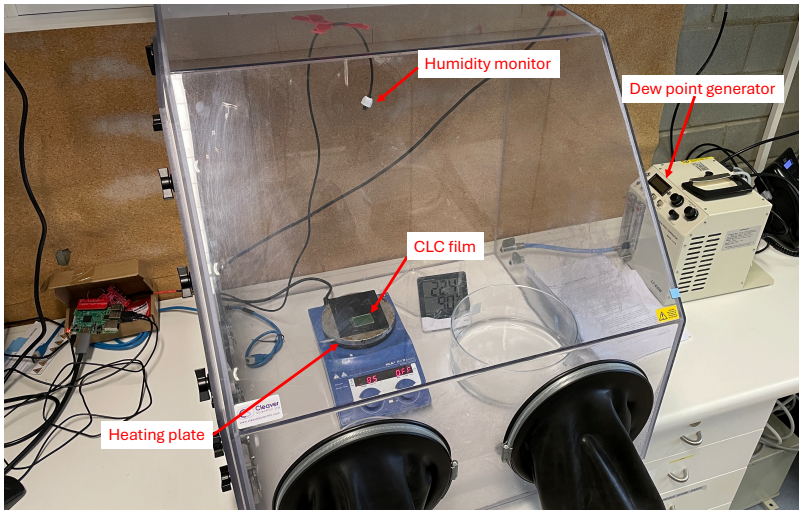

Figure S8. In-house-made humidity chamber setup. 85% humidity is provided by the dew point generator and 85 °C temperature is provided by the hot plate. The chamber is sealed and the samples are placed on the hot plate.

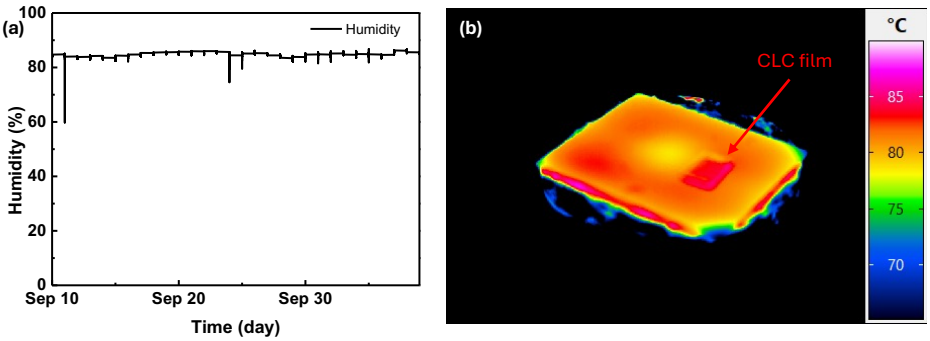

Figure S9. (a) Humidity monitoring results during testing, and (b) temperature results of the heated platform calibrated by the IR camera.

2 Generating non-spectral colours with CLCs on solar cells

2.1 Thermochromic and Polymerisable CLC Mixture for Colour Pixels

In order to obtain non-spectral colour solar cells, we use millimeter-scale size colour pixels from different spectral colours to mix non-spectral colour, which works on the same principle as in display technology. So we formulate a wide temperature range thermochromic and photopolymerizable liquid crystal mixture by incorporating benzoic acid derivatives, see Fig. S10. Benzoic acid based LC mesogens can broaden the temperature range of thermochromic properties of CLC mixtures with reversible responses[38]. We optimized the cholesteric phase range of the mixture using the Schröder-van Laar equation. Different amounts of benzoic acid derivatives are added to the mixture to expand the cholesteric phase temperature range, while avoiding excess concentrations that could result in phase separation. At the same time, the selective reflection of this eutectic mixture can be tuned across the full visible spectrum by varying the temperature. The composition of the final mixture used is given in Table S2.

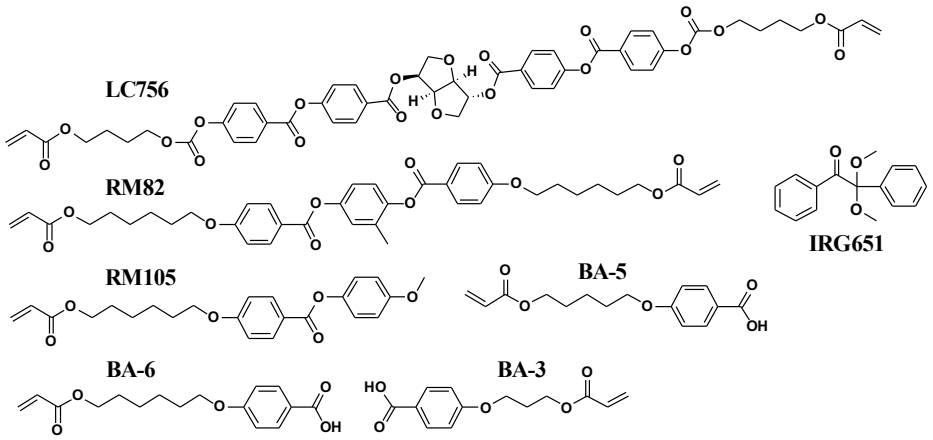

Figure S10. Chemical structures of monomers used to prepare the pixellated non-spectral film.

Table S2. Composition of CLC mixture used to prepare the pixellated non-spectral colour film.

RM82 (wt.%)	RM105 (wt.%)	BA-3 (wt.%)	BA-5 (wt.%)	BA-6 (wt.%)	LC756 (wt.%)	Irg651 (wt.%)
13	38	6.45	17.2	19.35	5	1

2.2 Optical Characterisation of Thermochromic and Polymerisable CLC-Mixture

The CLC phase of the polymerisable thermochromic mixture is characterized using POM with a cooling rate of 1 °C/min, as shown in Fig. S11. Above 66 °C, the mixture transitions to the isotropic phase, while between 66 and 10 °C, it exhibits the CLC phase. Notably, crystallization of mixture components was observed at 19 °C under fast cooling conditions. Similar to conventional thermochromic liquid crystals, the colour of the mixture redshifts when cooled from a high temperature to a low temperature. Retroreflection spectra are measured using a spectrophotometer, revealing that across the 56 °C wide cholesteric temperature range, the retroreflection peak redshifts on cooling from 461 nm to 685 nm. The observed working range exceeds 220 nm.

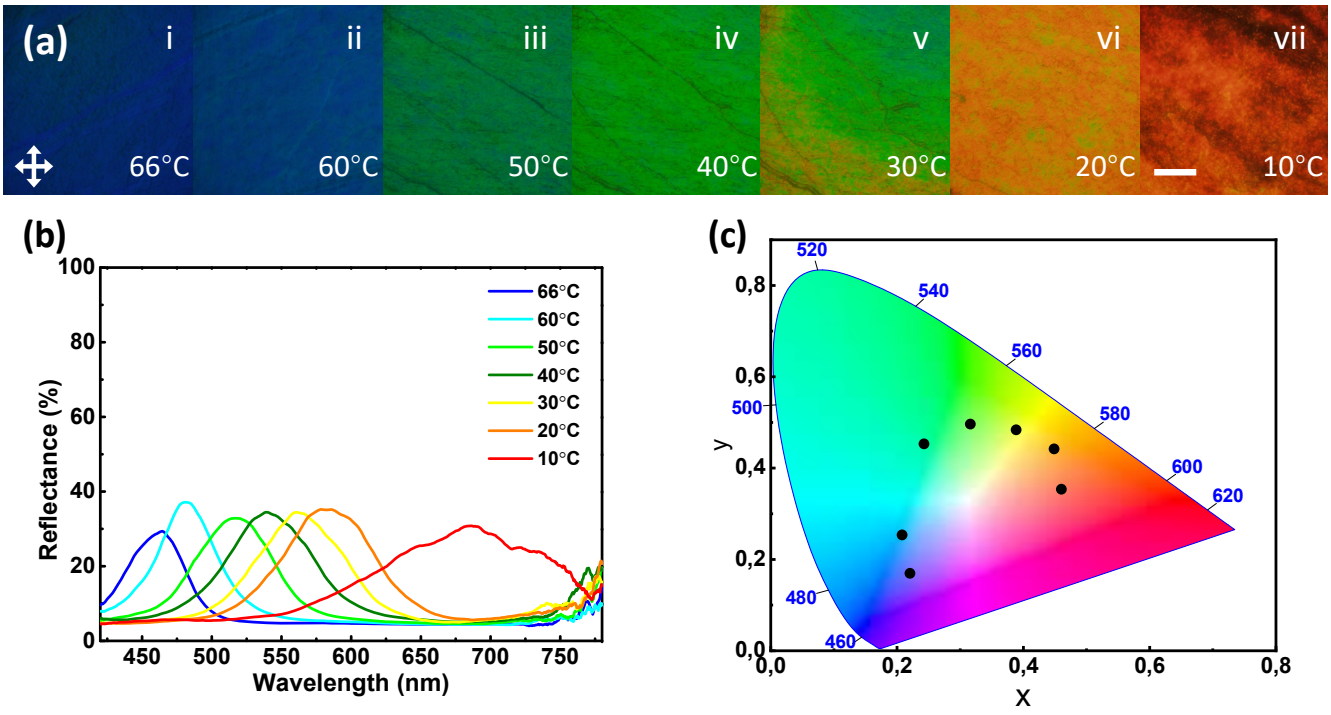

Figure S11. (a) Reflection POM images and (b) reflection spectra of polymerisable temperature-sensitive mixture upon cooling from 66 to 10 °C, at a cooling rate of 1 °C/min. (c) Colour coordinates (black dots) of the mixture in the CIE 1931 2° chromaticity diagram obtained according to the reflection spectra. Scale bar: 200μm.

2.3 *JV*-curves of the Solar Cells Before and After Pixellated CLC without and with *EQE* Correction

Fig. S12 shows the uncorrected and corrected JV performance under illumination for the best pixellated solar cell. Note that Fig. S12b is the same as Fig. 3f reprensented here for ease of comparison.

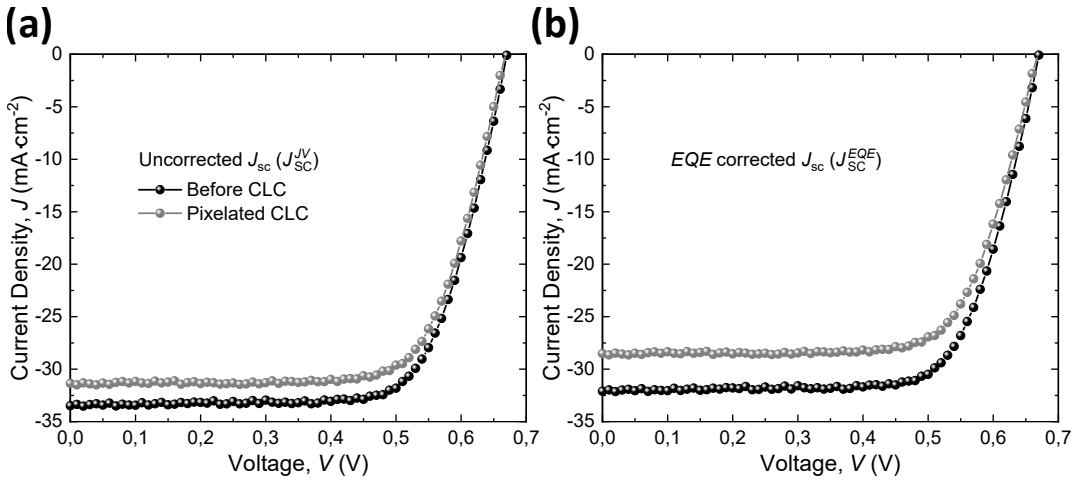

Figure S12. *JV*-curves of the best solar cell before and after pixellated CLC colouring shown in Fig. 3 (a) without and (b) with J_{SC}^{EQE} correction.

2.4 Statistical Analysis of Solar Cells Performances Before and After Pixellated CLC Coating

Fig. S13 shows the statistical analysis of solar cells before and after pixellated CLC coating. Note that J_{SC}^{JV} of these solar cells are not corrected with J_{SC}^{EQE}. Overall, it is obvious that the decrease in PCE after pixellated CLC is driven by the decrease in J_{SC}, as expected.

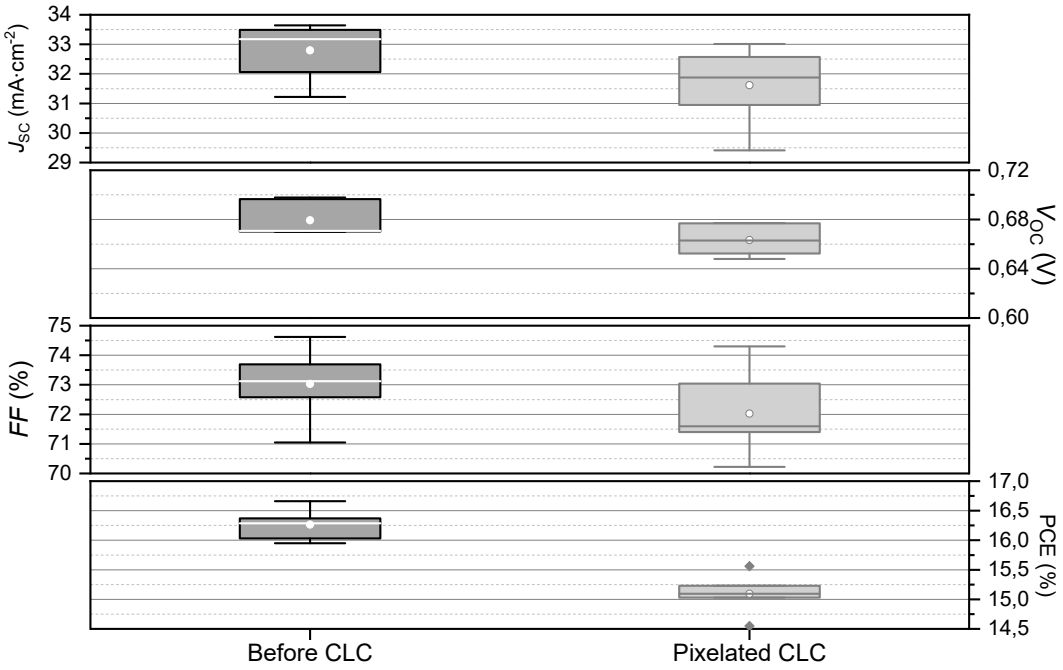

Figure S13. Boxplot of the performances of six solar cells before and after pixellated CLC colouring layers for the statistical analysis. It is important to note that J_{SC}^{JV} of solar cells are not corrected with J_{SC}^{EQE}.

2.5 Optical Characterisation of Polymerised and Pixellated CLCs on Solar Cells

The mixture is polymerized using two photomasks at 66 °C, 50 °C, and 10 °C sequentially. The reflection wavelengths of the three pixels after polymerization are measured by a spectrophotometer, as shown in Fig S14 (a). The reflection spectra of the polymerized pixellated films at 50 °C and 10 °C exhibit variations compared to the spectra of the unpolymerised mixture. This discrepancy arises from the consumption of mesogenic monomers during polymerization at 66 °C, leading to an alteration in the composition of the residual mixture. Consequently, slightly different reflection bands emerge at identical temperatures.

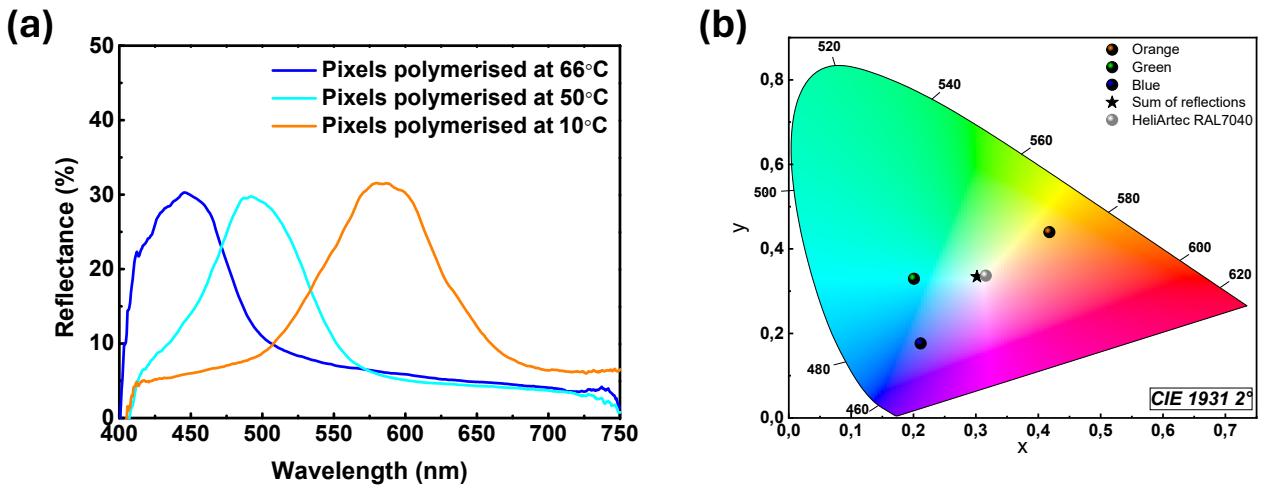

Figure S14. (a) Reflection spectra of three polymerised pixels. (b) Colour coordinates in the CIE 1931 2° chromaticity diagram of the three polymerised pixels (black dots filled with the respective colour) and the sum-up result (black star), as obtained from the reflection spectra, compared to the commercially available grey PV module RAL 7040 from HeliArtec (grey dot).

2.6 *EQE* Spectra of Individual Colour Pixels on a Solar Cell

The *EQE* spectra, from the individual colour pixels were measured using a μ*EQE*-setup with a spot size of ∼400 μm, is shown with the yellow dots (*EQE* measurement spot) in Fig. S15a. As a reference, a spectrum was acquired outside the pixellated region, that is on the bare solar cell. The resulting spectra are shown in Fig. S15b. Compared to the bare solar cell, each pixel's *EQE* spectrum additionally shows a dip around the wavelength range that corresponds to the respective pixel's colour.

2.7 Photographs of Solar Cell with Christmas Tree Pattern

The procedure for making a Christmas tree patterned solar cell in Fig. S16 is as follows: The mixture is dripped onto the solar cells at 50 °C, then covered with glass and left to anneal for 5 mins. A pre-designed photomask was placed on the glass surface and a handheld UV-LED system is used for photopolymerisation. After 10 s UV exposure with an intensity of 30 W/cm^2, the sample was cooled down to 40 °C at 5 °C/min. After stabilisation for 5 mins, the first photomask was replaced by a second photomask, followed by 10 s of photopolymerisation. Finally, the photomask was removed and the sample was cooled down to 10 °C for another 10 s UV exposure.

2.8 Photographs of Pixellated CLC Films under Different Illuminations and Backgrounds from Different Angles

The appearance from different angles of the same sample as in Fig. 4 is studied by photographing it from a set of different angles, from normal incidence to $\alpha = 60°$. The results are displayed in Fig. S17. All photos are taken in the same scene and the distance from the sample to the camera is approximately constant. The sample on the wooden door is imaged over a short distance of about 0.2 m, while the sample on the outdoor wall and door outside are studied at approximately 6 m distance. The sample blue shifts when α is increased.

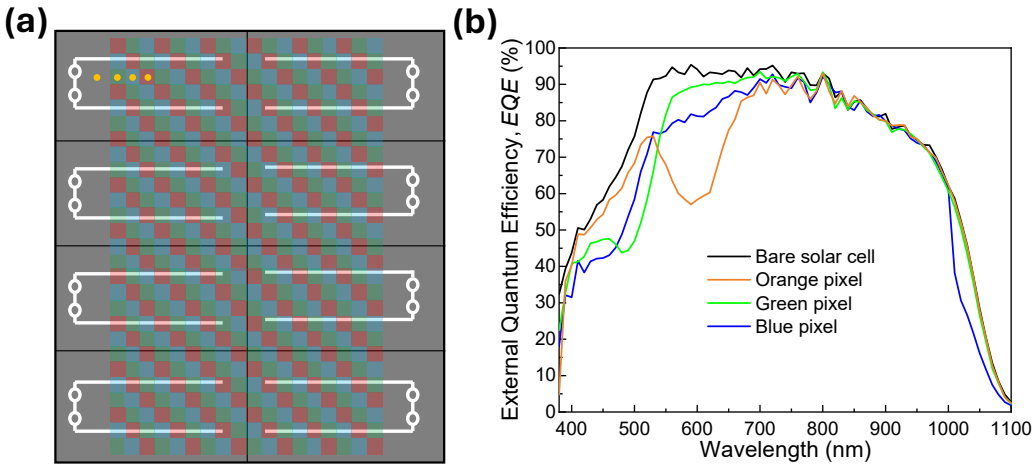

Figure S15. a) An in-house built μ*EQE*-setup has been employed for the measurement of solar cell performance at individual colour pixels, in which the μ*EQE* measurement spot has been shown with yellow dots. Since the measurement spot of the regular *EQE*-setup is larger than the individual pixels in the CLC film, we have employed μ*EQE*-measurement to reduce the spot size far below 1 mm in diameter (∼400 μm). b) *EQE*-characteristic of the individual pixel is shown.

Clearly, the colour responses from *EQE* are in line with the reflection data shown in Fig. S14.

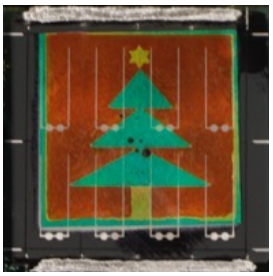

Figure S16. Solar cell with Christmas tree pattern.

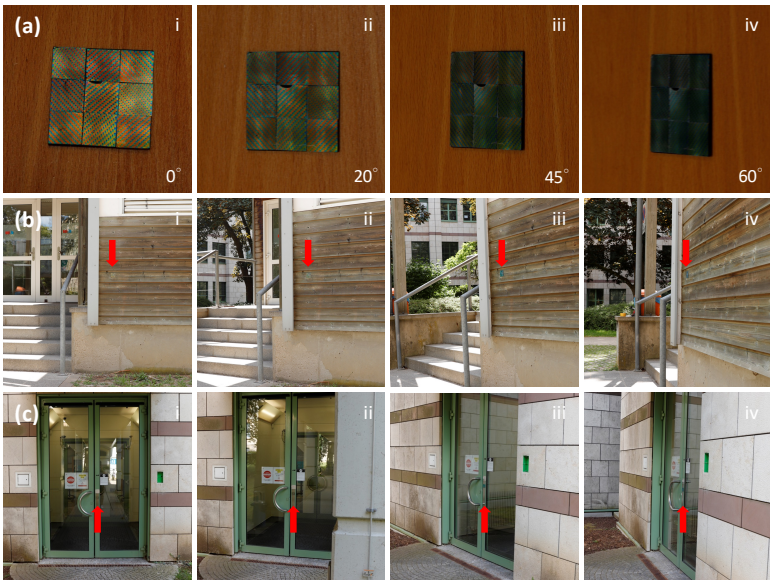

Figure S17. Photographs of the same pixellated film under different illumination conditions with different viewing angles. (a) Indoor photography under diffuse white light. The sample is 0.2 m away from the camera. (b) Outdoor photography under diffuse white light on a sunny day around the afternoon. Sunlight is incident on the sample from the left. The sample is 6 m away from the camera. (c) Outdoor photography under diffuse white light on a sunny day around the afternoon. The sun is blocked by the building. The sample is 6 m away from the camera. From i to v the photography angles are normal, 20°, 45°, and 60°, respectively.

3 Solar cells with temperature responsive colouring over a narrow range of temperatures

3.1 Chemical Formulation of Temperature sensitive CLC Mixtures

The composition of the CLC mixture used for the temperature sensitive colouring of the solar cells is given below. A sample of temperature-sensitive CLC mixture (components in Supplementary Fig. S18, compositions in Supplementary Table S3) is investigated with respect to its phase sequence by DSC, see Supplementary Fig. S19. Around 3–5 mg is placed in a crimped DSC aluminum pan, and a program with subsequent heating to 50 °C at 5 °C/min, cooling back to 20 °C at 5 °C/min, is carried out under nitrogen environment. The DSC indicates that above ∼ 37 °C the mixture is in the isotropic phase, between 37 and 28 °C it is in the cholesteric phase, and at ∼ 28 °C on cooling it undergoes a phase transition to what may be a smectic A phase.

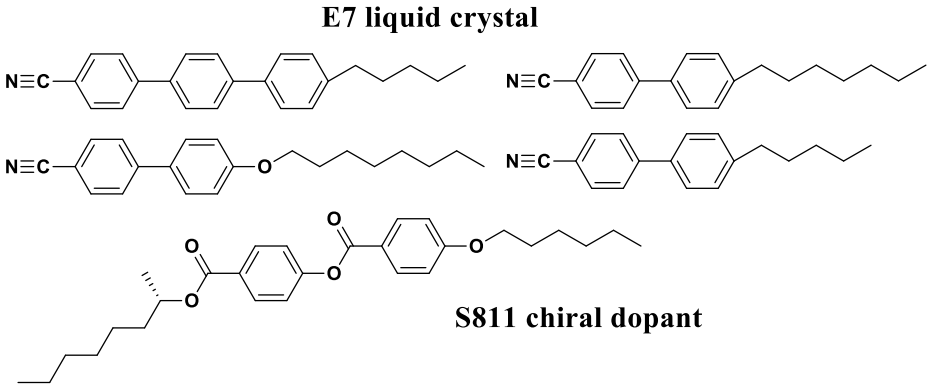

Figure S18. Chemical structures of materials used to prepare the temperature-sensitive colour mixture.

Table S3. Compositions of CLC mixture used to prepare the temperature-responsive colour mixture.

E7 (wt.%)	S811 (wt.%)
70	30

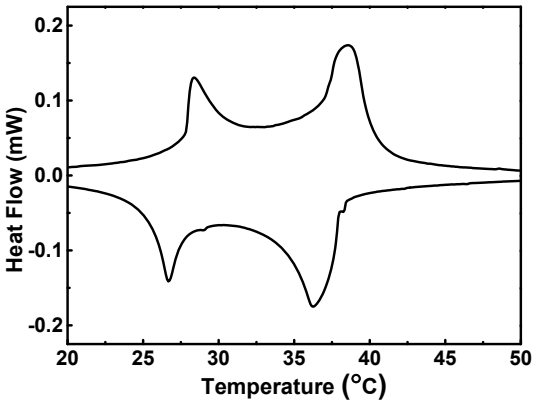

Figure S19. DSC curves of the temperature-sensitive mixture from 20 to 50 °C measured at a heating/cooling rate of 5 °C/min. The left peak is likely a transition from a smectic to the cholesteric phase, and the right peak indicates the phase transition from the cholesteric to the isotropic phase.

3.2 Polarised Microscopy Images and Photographs of Temperature Responsive CLCs on Solar Cells over a Range of Temperature

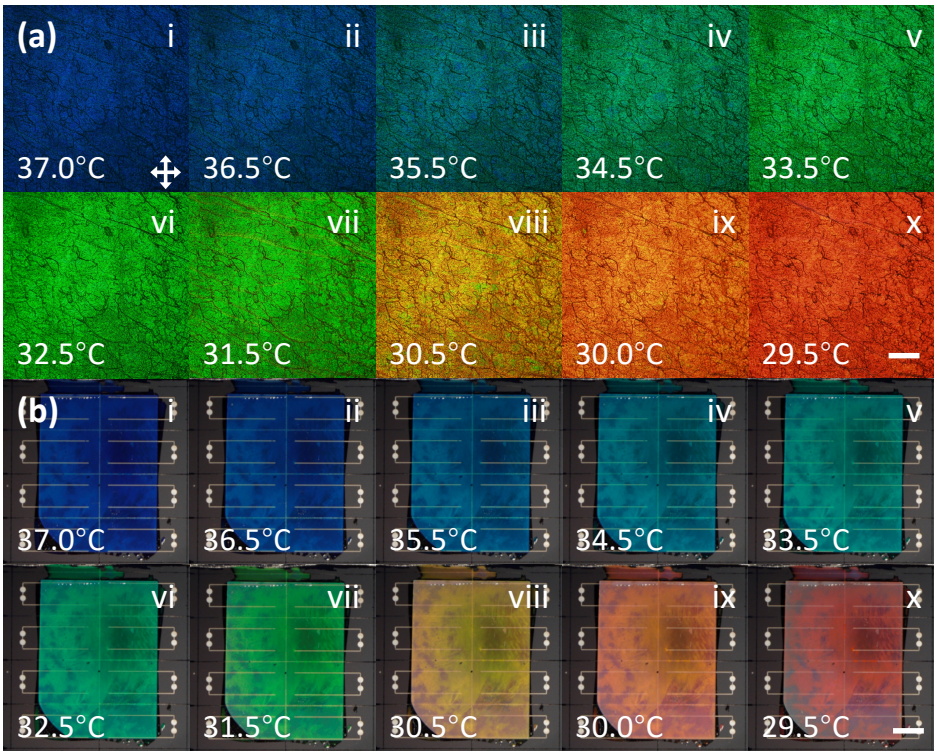

Figure S20. (a) POM (scale bar: 200 μm), and (b) camera (scale bar: 1 cm) images of the temperature-sensitive solar cell as the temperature decreased from 37 °C to 29.5 °C, respectively.

3.3 PV Performance of the Solar Cell with Temperature Responsive CLCs

Fig. S21 shows the uncorrected and corrected *JV* performance under illumination at 25°C and 31.5°C, which corresponds to a green colour. The change in voltage is due to the increase in temperature.

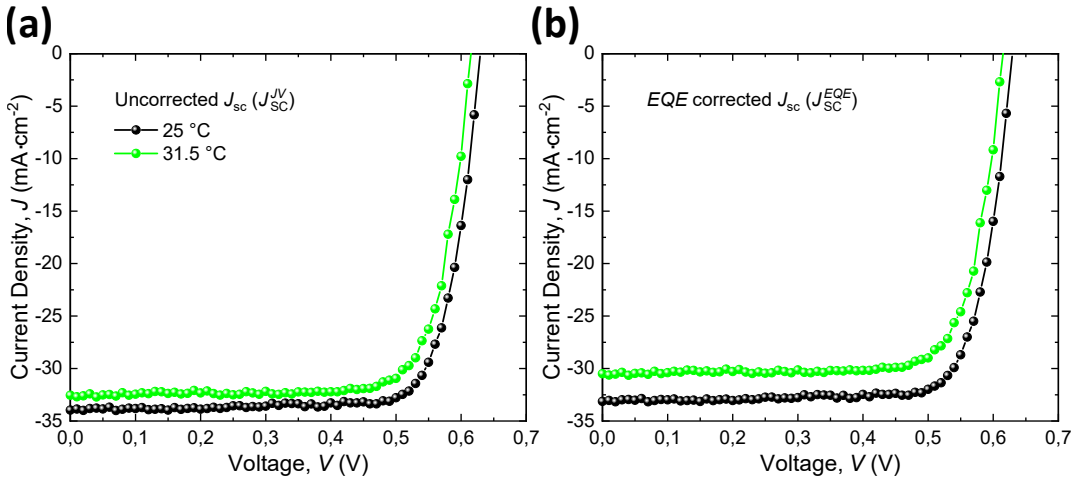

Figure S21. *JV*-curves of a temperature responsive CLC coated solar cell at two different temperatures shown in Fig. 5 (a) without and (b) with J_{SC}^{EQE} correction.

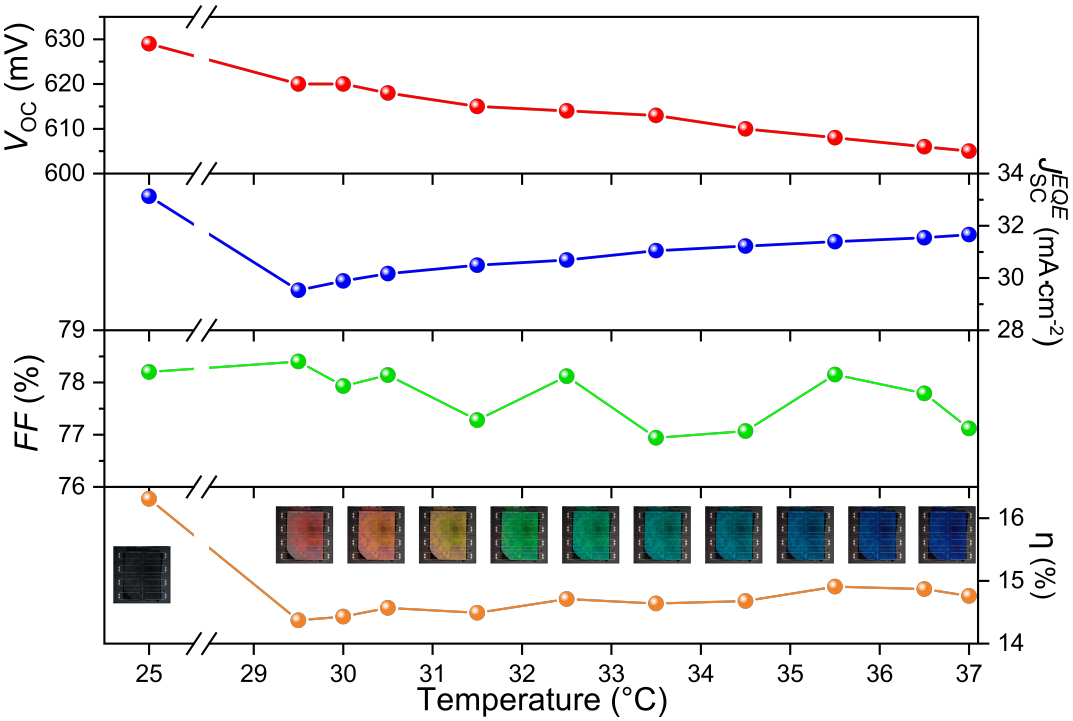

Figure S22. The effect of temperature change on the *JV*-parameters of the solar cell after the deposition of temperature responsive CLCs. As expected, there is a gradual decline in V_{OC} as the temperature rises, which is a characteristic of solar cells. However, J_{SC} experiences a sudden drop from 25°C to 29.5°C due to the red colour response in CLC, resulting in the lowest efficiency. It then gradually increases with the temperature rise due to the colour changing towards blue.